THE JOURNAL OF BIOLOGICAL CHEMISTRY VOL. 285, NO. 8, pp. 5859–5867, February 19, 2010

ATP Hydrolysis in Eg5 Kinesin Involves a Catalytic Two-water Mechanism*[S]◆

Received for publication, September 29, 2009, and in revised form, November 16, 2009 Published, JBC Papers in Press, December 15, 2009, DOI 10.1074/jbc.M109.071233

Courtney L. Parke, Edward J. Wojcik, Sunyoung Kim[1], and David K. Worthylake

From the Department of Biochemistry and Molecular Biology, Louisiana State University Health Sciences Center, New Orleans, Louisiana 70112

Motor proteins couple steps in ATP binding and hydrolysis to conformational switching both in and remote from the active site. In our kinesin·AMPPPNP crystal structure, closure of the active site results in structural transformations appropriate for microtubule binding and organizes an orthosteric two-water cluster. We conclude that a proton is shared between the lytic water, positioned for γ-phosphate attack, and a second water that serves as a general base. To our knowledge, this is the first experimental detection of the catalytic base for any ATPase. Deprotonation of the second water by switch residues likely triggers subsequent large scale structural rearrangements. Therefore, the catalytic base is responsible for initiating nucleophilic attack of ATP and for relaying the positive charge over long distances to initiate mechanotransduction. Coordination of switch movements via sequential proton transfer along paired water clusters may be universal for nucleotide triphosphatases with conserved active sites, such as myosins and G-proteins.

In a wide variety of protein machines, the binding and hydrolysis of ATP are chemically coupled to large scale conformational changes that occur within and distant from the nucleotide site, resulting in force generation and movement. Bimolecular motors, like kinesins (1, 2), and proteins not conventionally considered motors, such as DNA-modifying enzymes, use this principle of mechanotransduction to perform their cellular roles. However, direct cause-and-effect linkage between the catalytic steps and powered structural changes in these proteins has not been established, principally as the deprotonation partner in the initial chemical step of protein-driven ATP hydrolysis is not known.

Within kinesins, as well as myosins and G-proteins, common sequence motifs, such as switch I, switch II, and the P-loop, organize into an active site that can accelerate NTP hydrolysis. It is well accepted that the nucleophile for catalysis is a water molecule and that protonation and deprotonation events are at the core of this acid-base reaction. Upon substrate binding, the initial chemical step is that a catalytic base abstracts a proton from the lytic water. The resulting hydroxide ion attacks the substrate at the γ-phosphate and alters the partial charge distribution between the γ- and β-phosphate groups. The β-γ-phosphoanhydride bond is cleaved upon the shift in electron charge within the substrate, and the reaction products, a nucleotide diphosphate leaving group and an inorganic phosphate (P_i), are formed.

Elusive for kinesins specifically and other ATPases in general is experimental identification of the catalytic base. The chemical nature of the base defines how catalysis in motor proteins can be accelerated, controlled, or reversed. The archetypal model of protein-mediated ATP hydrolysis predicts that the proton acceptor should be a conserved amino acid side chain and that the proton-donating and proton-accepting groups are in close proximity. However, protein crystallographic models (3) have not identified an obvious proton acceptor within 5 Å of the phosphate ester linkage of ATP. Thus, two alternate proposals have been put forth: substrate-assisted catalysis, in which a proton of the attacking water molecule is transferred to an oxygen of the γ-phosphate (4), and a proton relay mechanism in which a water network spanning the distance between conserved residues and substrate provides a proton shuttle (5). Implicit within the latter proposal is that the distance between the acid-base pair can be increased by water molecules. Discrimination between these proton transfer models is necessary for not only understanding the mechanism of ATP hydrolysis proper but also for describing how events at the active site are transmitted to distal parts of the protein.

Here we have determined the crystal structure of the wild-type motor domain of human Eg5 kinesin in a prehydrolytic state, trapped by the non-hydrolyzable analogue AMPPNP.[2] This study provides the first experimental observation of the catalytic base for any nucleotide triphosphatase (NTPase) and the first atomic details regarding the prehydrolysis state for any motor protein. Several observations in our data support these assignments. The electron density around the bound nucleotide (see Fig. 1*a*) cradles three phosphate groups in the active site, and the γ-phosphate is in a tetrahedral geometry. Second, both switch regions are in a closed conformation (see Fig. 1*b*)

* This work was supported, in whole or in part, by National Institutes of Health Grant GM066328 (to E. W.). This work was also supported by funding from Louisiana Board of Regents grants (to D. W. and to S. K.).

◆ This article was selected as a Paper of the Week.

The atomic coordinates and structure factors (code 3HQD) have been deposited in the Protein Data Bank, Research Collaboratory for Structural Bioinformatics, Rutgers University, New Brunswick, NJ (http://www.rcsb.org/).

[S] The on-line version of this article (available at http://www.jbc.org) contains supplemental Fig. S1, Tables S1 and S2, and Movies S1 and S2.

[1] To whom correspondence should be addressed: 1901 Perdido St., New Orleans, LA 70112. Tel.: 504-568-2019; Fax: 504-568-3370; E-mail: skim3@lsuhsc.edu.

[2] The abbreviations used are: AMPPNP, 5′-adenylylimidodiphosphate; NTPase, nucleotide triphosphatase; MT, microtubule; MES, 4-morpholineethanesulfonic acid; PIPES, 1,4-piperazinediethanesulfonic acid; cryo-EM, cryo-electron microscopy.

and linked by a salt bridge, revealing an ordered water network spanning the distance from an interswitch salt bridge to the nucleotide γ-phosphate. Lastly, structural elements required for microtubule (MT) binding have distinct conformational organizations and molecular interactions not previously observed. This initial set of structural and chemical isomerizations necessary to prime ATP hydrolysis and mechanotransduction in kinesins is likely conserved in myosin, another major superfamily of motor proteins. Our data also provide a mechanistic model for how transmission of a proton across a water network disrupts an interswitch salt bridge, thereby promoting a second major conformational transition.

EXPERIMENTAL PROCEDURES

Protein Expression and Purification—The gene encoding human Eg5 (6) (residues 1–369) was cloned into pET28a and transformed into the BL21(DE3) Rosetta™ host strain. Cells were grown at 37 °C to an $A_{600\ nm} = 0.6$. The temperature was reduced to 27 °C, and 0.5 mM isopropyl-1-thio-β-D-galactopyranoside was added. Cells were harvested after 5 h, resuspended in Buffer A (10 mM MES, pH 6.0, 20 mM NaCl, 5% glycerol, 1 mM EGTA, 1 mM EDTA) supplemented with phenylmethylsulfonyl fluoride, DNase I (Roche Applied Science), and RNase A (Sigma), and lysed using an Emulsiflex-C5 (Avestin). Lysate was centrifuged at 184,250 × *g* for 45 min, and the supernatant was loaded onto a 5-ml SP Sepharose column pre-equilibrated with Buffer A. The protein was eluted by a NaCl gradient, concentrated to 13 mg/ml, and incubated with apyrase and 4 mM $CaCl_2$ to remove bound ADP. The protein solution was centrifuged for 15 min at 26,000 × *g*, and the supernatant was loaded onto a 26/60 Sephacryl 200 (GE Healthcare) column equilibrated with 10 mM MES, pH 6.0, 5% glycerol, 175 mM NaCl, 2 mM dithiothreitol. Pooled protein was diluted with 27 mM Tris, pH 8.0, 5% glycerol, 2 mM dithiothreitol, 1.3 mM EGTA, 1.3 mM EDTA to ~40 mM NaCl and loaded onto a 8-ml SourceQ column equilibrated with 10 mM Tris, pH 8.0, 40 mM NaCl, 5% glycerol, 2 mM dithiothreitol, 1 mM EGTA, 1 mM EDTA. The protein was eluted with a NaCl gradient. Purified Eg5 was identified via SDS-PAGE, concentrated, buffer-exchanged to 50 mM PIPES, pH 6.8, 2 mM $MgCl_2$, 1 mM EGTA, 2 mM dithiothreitol, 50 mM KCl, 5% glycerol, 1 mM AMPPNP, and stored at −80 °C. Activity assays (6) indicate that apyrase-treated Eg5 protein efficiently hydrolyzes ATP *in vitro*.

Crystallization, Data Collection, and Data Processing—Crystals obtained with Hampton Crystal Screen Cryo™ solution 42 were used to streak seed drops containing a 1:1 ratio of protein to well solution (40 mM KH_2PO_4, 20% glycerol w/v, 15% polyethylene glycol 8000 w/v). Crystals were grown by vapor diffusion at 4 °C in hanging drops. Rectangular crystals appeared overnight and were allowed to grow for several days before flash-freezing in LN_2. Diffraction data (Table 1 and supplemental Table S1) were collected at 100 K using a Bruker MICROSTAR x-ray generator equipped with HELIOS optics and a PROTEUM 4K PLATINUM 135 CCD camera and were integrated and scaled with PROTEUM2 software (Bruker AXS). Crystals belong to space group P2(1) with cell parameters $a = 60.50$ Å, $b = 71.44$ Å, $c = 94.85$ Å, and $\beta = 98.86°$. Volume considerations indicated that two Eg5 molecules existed in the crystal asymmetric unit.

TABLE 1
X-ray refinement statistics

Resolution (Å)	2.19
R_{work}[a]/R_{free}[b]	0.224/0.262
Number of atoms	5,834
Protein	5,484
Ligand/ion	69
Water	281
***B*-factors**	28.59
Protein	28.78
Ligand/ion	22.68
Water	26.35
r.m.s.[c] deviations	
Bond lengths (Å)	0.008
Bond angles (°)	1.61
φ/ψ	
Most favored/additional allowed/disallowed (%)	91.7/8.1/0.2

[a] $R_{work} = \Sigma_h|F_{oh} - F_{ch}|/\Sigma_h|F_{oh}$, where F_{oh} and F_{ch} are the observed and calculated structure factor amplitudes for the reflection *h*. Working set includes 36,987 reflections.
[b] *R*-factor calculated for 4,140 reflections that were chosen randomly and not included in the refinement.
[c] r.m.s., root mean square.

Structure Solution and Refinement—The Eg5·AMPPNP complex structure was determined using the program AMoRe (7) and molecular replacement. The search model was molecule A of the Eg5·ADP·monastrol complex (Protein Data Bank (PDB) ID 1X88) without associated waters, ADP, Mg^{2+}, and monastrol. These coordinates are also missing switch II cluster residues 272–286. Using data in the range 8–3.5 Å and a sphere of 25 Å, the rotation function yielded two clear solutions. The translation function verified that the top two rotation function orientations were correct. Rigid-body fitting in AMoRe using data in the range 8–3.5 Å yielded an R_{cryst} of 48.2. At this point, 15 steps of CNS (8) rigid-body refinement using data from 25 to 2.42 Å yielded $R_{cryst} = 49.5$, $R_{free} = 48.8$. Next, a 5,000 K slow cool-simulated annealing using torsion angle dynamics produced coordinates with $R_{cryst} = 40.0$, $R_{free} = 45.6$ for 25–2.42 Å data. Inspection of initial $2F_o - F_c$ and $F_o - F_c$ maps indicated significant differences primarily in the two switch regions. These portions of the model were removed, and data were extended to 2.19 Å. Successive rounds of manual model building with O (9) and automated refinement were performed. When the model (not including waters, nucleotide, or Mg^{2+}) was essentially complete, the CCP4 (10) program ACT was used to guide the application of non-crystallographic symmetry restraints. Non-crystallographic symmetry was applied to 34 residues in each of the two molecules. At a very late stage in model building, the coordinates and topology/parameter files for AMPPNP were acquired from Hic-Up (11), and the nucleotide and Mg^{2+} were positioned into the active sites.

The final model contains residues 17–366 for each molecule of the asymmetric unit, 281 waters, two AMPPNP molecules, two Mg^{2+} ions, and one inorganic phosphate (Table 1 and supplemental Table S1). To determine whether we had inappropriately applied non-crystallographic symmetry, a 5,000 K slow cool-simulated annealing refinement using torsion angle dynamics was performed on the final model without the use of non-crystallographic symmetry restraints. The root mean square difference between the two Eg5 molecules after this

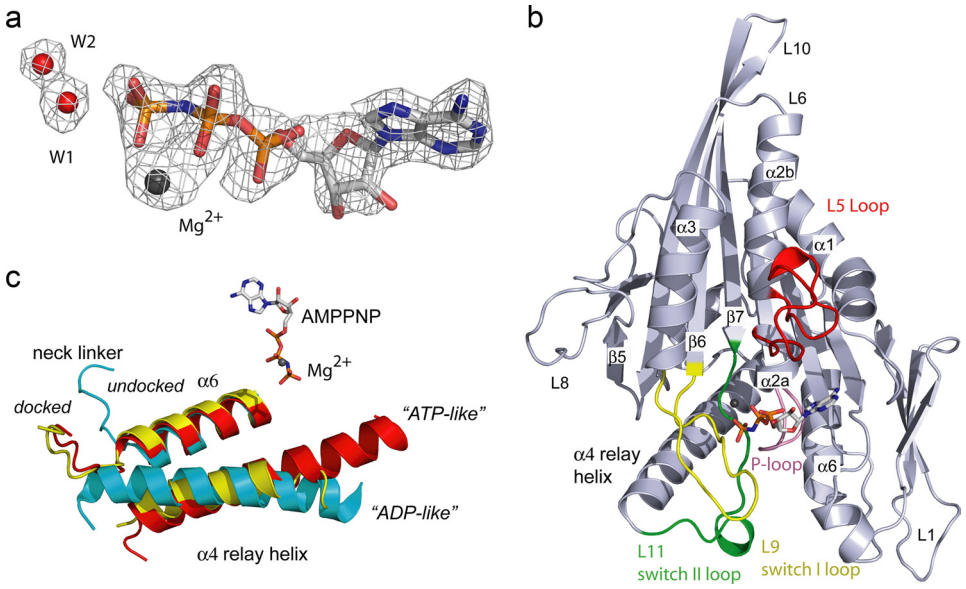

FIGURE 1. **Structural features of Eg5·AMPPNP.** *a*, $F_o - F_c$ simulated annealing omit density map contoured at 3σ surrounds the AMPPNP, Mg^{2+}, **W1,** and **W2**. *b*, highlighted in the Eg5·AMPPNP complex are L9 (*yellow*) containing switch I, L11 (*green*) containing switch II, the P-loop (*pink*), and the L5-loop (*red*), which is involved in binding allosteric inhibitors. AMPPNP and Mg^{2+} (*dark sphere*) are also shown. *c*, comparison of α6, α4, and the neck linker of Eg5·AMPPNP (*red*), Eg5·ADP (*cyan*), and Kif1A·AMPPNP (*yellow*) after superimposing the structures (see "Experimental Procedures").

refinement was 0.64 Å for all Cα atoms and 0.10 and 0.28 Å between Cα atoms from regions that include switch I (residues 217–238) and switch II (264–281) of each Eg5 molecule.

Figures and Morphs—Figs. 1–4 and supplemental Table S2 were made using PyMOL (12). Cα atoms of residues 102–111 of Eg5 and the equivalent residues from Eg5·ADP (PDB ID 1II6), Kif1A·AMPPNP (PDB ID 1VFV), and myosin II·ADP·vanadate (PDB ID 1VOM) were used for aligning coordinates for Figs. 1 and 2 and also coordinates used to produce supplemental Table S2. The AMPPNP-bound-to-ADP-bound movies (supplemental Movies S1 and S2) were made using the RigiMOL add-on in PyMOL, as well as the eMovie (13) plug-in. The start state included the Eg5·AMPPNP structure (PDB ID 3HQD), and the end state was Eg5·ADP (PDB ID 1II6). For clarity, the missing portion of the Eg5·ADP switch II loop was assembled in Swiss-Pdb Viewer and energy-minimized.

RESULTS

Closed Active Site—To our knowledge, there is no prior published crystallographic observation of the fully closed conformation of an active site or of a γ-phosphate-sensing mechanism for kinesin motor proteins. Kinesins, in common with myosins, are thought to undergo an ATP-induced conformational transition in which the switch regions flanking the active site shift from "open" to "closed" states (14, 15) with the open state resembling the ADP-bound conformation. Indeed, numerous NTPases employ a γ-phosphate-sensing mechanism that alters their molecular conformations dependent upon the presence or absence of the γ-phosphate. The closed state of NTPases, in which critical determinants have been correctly positioned, is competent for supporting nucleotide hydrolysis, whereas the open state is not.

Accordingly, the conformations of switch regions in the closed state of kinesins should be structurally distinct from either ADP-bound protein or the initial ATP·kinesin collision complex. Although the overall architecture of the Eg5·AMPPNP complex is akin to that of other microtubule motors (Fig. 1*b*), there are differences among the loops and helices surrounding the core β-sheet; these include L5, L9 (containing the ^{229}NAYSSR^{234} switch I sequence (16)), α3, L11 (containing the ^{265}DLAGSE^{270} switch II sequence (16)), α4, L12, and α6 (Fig. 1*b*). These regions are dissimilar from ADP-bound Eg5, exhibit two novel structural features that distinguish them from the structures of other kinesins bound to ATP analogues or transition state mimics (supplemental Table S2), and are consistent with expectations of a closed, catalytically competent state.

First, the switch I conformation in Eg5·AMPPNP (Fig. 2*a*) adopts a closed conformation, unique for kinesins but previously seen in myosins (17). In the Eg5·ADP structure (18), switch I residues 231–234 adopt a helical conformation that is 4 Å removed from the location of the (absent) γ-phosphate (Fig. 2*a*). The C terminus of α3 (residues 221–226; Fig. 2*a*), immediately preceding switch I, is unwound in the Eg5·AMPPNP structure in comparison with the Eg5·ADP structure. Unwinding of the α3 C terminus increases the length of the switch I loop, fosters interactions of the NAYSSR motif observed at the active site, and rotates the α3 helix slightly (~11°, Fig. 2*a*) relative to the core β-sheet. As the switch I region of a kinesin had never been observed in a conformation analogous to that of a closed myosin switch I, it has been hypothesized that kinesin switch I functions differently from that of myosin (15). However, our data confirm that the switch I of kinesins and myosin operates via closely related mechanisms, with each adopting a similar switch I conformation (Fig. 2*b*) that is required to fully enclose the nucleotide-binding site.

Second, the switch II region in the Eg5·AMPPNP complex assumes a completely closed conformation (Fig. 2*c*), and the switch II loop interacts with switch I and the nucleotide γ-phosphate. Comparison of the ADP-bound, ATP analogue-bound, and transition state mimic-bound forms of kinesins (supplemental Table S2) does not show large changes in the secondary structure of switch II, and no large secondary structure changes are noted in this region of the Eg5·AMPPNP complex. However, for the first time in any wild-type kinesin crystal structure, the Eg5·AMPPNP structure features a completely ordered switch II loop (L11). The ordered switch II loop (Fig. 2*c*, *red*), which includes a short helical element formed by residues 272–275, is extended toward the active site. Residues in the switch II loop participate in H-bonding interactions with residues of switch I, the P-loop, α6, active site water molecules, and the nucleotide proper (see below). Because the switch II loop in Eg5

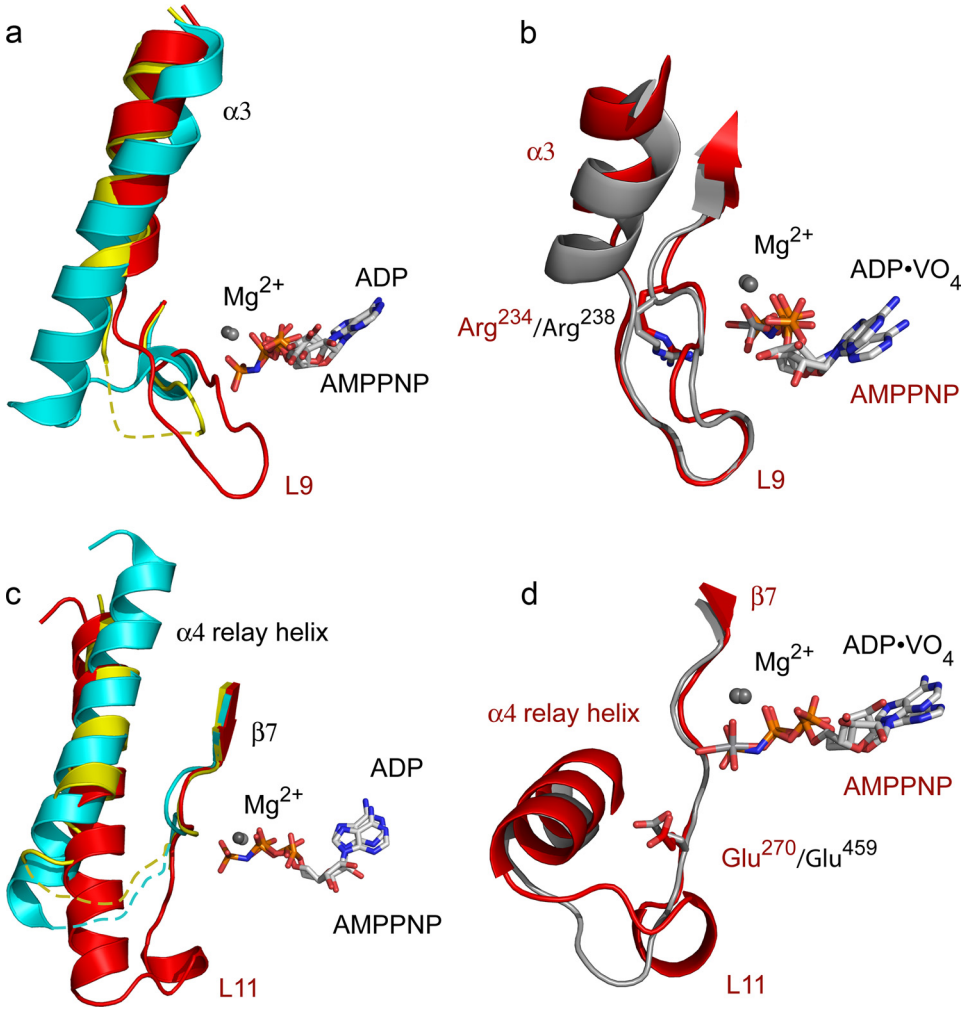

FIGURE 2. **Closed nucleotide-binding site.** Comparisons of the α3 helix and switch I loop (*a* and *b*) and of the relay helix and switch II loops (*c* and *d*) from representative kinesin and myosin structures are shown. *a*, differences in α3 and L9 between Eg5·AMPPNP (*red*) with the equivalent sequences of Eg5·ADP (*cyan*) and Kif1A·AMPPNP (*yellow*). Disordered residues are shown as *dashed lines*. Note that L9 of Eg5·AMPPNP approaches the nucleotide in this closed conformation. *b*, Eg5·AMPPNP (*red*) and myosin·ADP·vanadate (*gray*) have similar switch I loop conformations. Conserved switch I arginines are shown. *c*, relay helices and switch II loops of Eg5·AMPPNP (*red*), Eg5·ADP (*cyan*), and Kif1A·AMPPNP (*yellow*). L11 of Eg5·AMPPNP is ordered, and the relay helix is in an ATP-like position. *d*, Eg5·AMPPNP (*red*) and myosin·ADP·vanadate (*gray*) have similar switch II loop conformations. Conserved switch II glutamates are shown.

ADP-bound structures is disordered (supplemental Table S2), it appears that interactions provided by the γ-phosphate of AMPPNP have a stabilizing effect on these residues.

Propagated Changes at the Microtubule-binding Site—Interaction with microtubules is crucial to kinesin function, and the ATP-bound form of motor proteins is accepted as the conformational state in which microtubules are stably bound (19, 20) and in which forward motion is produced in dimeric forms of kinesin. Therefore, substrate binding to the active site should elicit distal structural changes at the MT-binding surface, and these microscopic changes have been probed using crystallography and cryo-EM techniques. The "ATP-like" or "helix-up" structural orientation of the switch II relay helix (α4) in kinesins (19), also observed in our Eg5·AMPPNP structure (Fig. 1*c* and supplemental Movie S1), has been correlated with the chemical state of the nucleotide bound to the motor domain. This ATP-like position differs from the "ADP-like" state as the N-terminal portion of α4 is rotated toward the nucleotide-binding site and the helix as a whole is shifted away from the central β-sheet. In the ATP-like position, α4 is shifted out of the plane of the α6 helix, allowing for neck linker docking against the core β-sheet.

Cryo-EM studies revealed that the α4 relay helix is also lengthened in kinesin·microtubule complexes (14, 21, 22). This lengthening has not uniformly been observed in the kinesin crystal structures in a presumed ATP-like state, prompting the suggestion that MT interactions are necessary for stabilizing a longer α4 helix (22, 23). Challenging this idea, the α4 helix in our crystal structure, found at the MT-binding face, agrees well in both length and orientation with cryo-EM densities of *Drosophila* Kinesin-5·AMPPNP·MT complexes (21). Comparison of and structural agreement between our data and this recent cryo-EM study (21) reveal that not only the orientation but also the length of the α4 helix is important for achieving a tight, AMPPNP-MT-bound state and is directly correlated with the stability of the switch II loop.

In addition, the fully ordered switch II region, only observed in the AMPPNP-form of Eg5, appears to organize additional residues into the α4 helix and alter the orientation of the relay helix. Coincident with these conformational changes is the observation of a novel network of H-bonding among residues of the switch II helix, the P-loop, and the α6 helix. Asn^{342} of α6, Arg^{274} of the switch II loop, and Gln^{106} of the P-loop form an H-bonding triad (supplemental Fig. S1). This interaction appears to stabilize the closed conformation of the switch II loop and may also serve as a mode of communication from the active site to the MT-binding surface.

Atomic Interactions in the Closed Active Site—The closing of the nucleotide-binding pocket produces changes critical for enzyme-catalyzed ATP hydrolysis. Three mechanistic outcomes result from the conformations adopted by switch regions and their adjacent secondary structures and drive toward a conclusion regarding the biochemical role of the switch elements. First, there is formation of an anticipated interswitch salt bridge (15) between the side chains of switch I Arg^{234} and switch II Glu^{270} that closes the active site (Fig. 3*a*). This Eg5 salt bridge is equivalent to a salt bridge between analogous residues in myosin switches, shown to be essential for closing the active site and ATP hydrolysis (24–26). The salt-

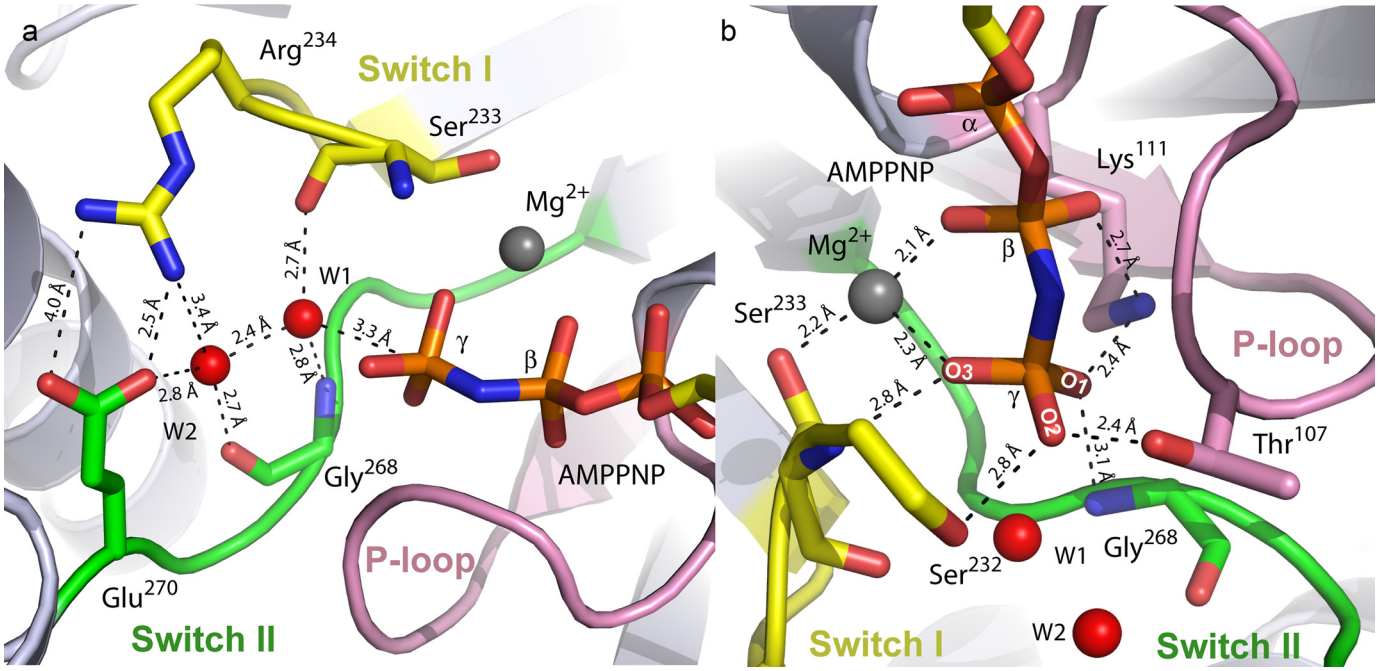

FIGURE 3. **Nucleotide-binding pocket of Eg5·AMPPNP.** *a*, waters **W1** and **W2** make extensive interactions with switch I residues Ser^{233} and Arg^{234} (*yellow*) and switch II residues Gly^{268} and Glu^{270} (*green*). Measured interatomic distances are shown. **W1** is 3.3 Å from the γ-phosphorus atom. *b*, oxygen atoms of the nucleotide γ-phosphate are coordinated by Mg^{2+}, switch I and switch II residues, and residues of the P-loop (*pink*).

bridge geometry seen in the myosin·ADP·vanadate (17) and our Eg5·AMPPNP substrate pockets has not been observed in other wild-type kinesin structures in which the salt bridge is not formed at all or which feature a salt bridge with different geometries and distances (23, 27, 28). These kinesin structures may represent intermediate states that precede an ATP-induced, fully closed conformation.

A second mechanistic outcome resulting from the closed conformations adopted by Eg5·AMPPNP switch elements is the observation of not one but two water molecules (Figs. 1*a* and 3, **W1** and **W2**) in the active site, one of which (**W1**) is coordinated by conserved switch residues and lies close to the scissile phosphate of AMPPNP. These two waters are present in each of the two Eg5·AMPPNP complexes in the crystal asymmetric unit with nearly identical orientations and with **W1**–**W2** separation distances in each complex of 2.41 and 2.43 Å. Furthermore, omit electron density maps show that the densities for all four of the water molecules are well formed and equal in size (data not shown), and the temperature factor values for these water molecules have been refined to below the average for waters within the structure.

The first water, **W1**, is oriented 3.3 Å from the γ-phosphorus atom in a nearly perfect "in-line" position for a nucleophilic role in catalysis (Fig. 3). This is the first observation of a water molecule proximal to the γ-phosphate of the kinesin substrate, and thus the lytic water, in these motor proteins. **W1** is coordinated by the amide carbonyl group of switch I Ser^{233}, the backbone amide group of switch II Gly^{268}, and a second water molecule, **W2**. Given the chemistry of the available moieties surrounding **W1**, we reach the unexpected conclusion that **W2** serves as the proton acceptor for the nucleophilic **W1** (see below). The second water is secured in the nucleotide pocket via the backbone oxygen of Gly^{268} and the side chain oxygen of switch II Glu^{270}. Thus, this active site water pair is positioned by a tight network of hydrogen bonds and bridges the distance between the γ-phosphate and the interswitch salt bridge. The advantage of such a hydrogen-bond network has been calculated for myosins, G-proteins, and F_1-ATPase (29–32) but never experimentally observed.

A third important feature of the closed active site is the extensive protein-mediated electrostatic stabilization and H-bonding of the bound nucleotide that are central features in enzyme-catalyzed nucleotide hydrolysis. These H-bonding interactions with the nucleotide, complex in nature and also large in number, can have two effects: polarization of the γ-phosphate P–O bonds and reduced Coulombic repulsion in preparation for an associative nucleophilic attack by the lytic water (below). Overall, there are also two active site residues that have three H-bonds. Switch I Ser^{233} and switch II Gly^{268} each have hydrogen bonds to the γ-phosphate of AMPPNP and to **W1**. Interactions with Mg^{2+} and **W2** form the third coordinations for Ser^{233} and Gly^{268}, respectively (Fig. 3*a*). There are also two functional groups that form bidentate ligations in the active site; Mg^{2+} tethers oxygens of both the γ-phosphates and the β-phosphates of the adenine nucleotide and Lys^{111} in the P-loop H-bonds with both the γ-phosphate and the β-phosphate.

In detail, the Eg5 switch elements form extensive H-bonding interactions with the β-γ bridging oxygen and γ-phosphoryl oxygens of AMPPNP and with the Mg^{2+} ion. The nitrogen of AMPPNP, a chemical substitute for the β-γ bridging oxygen atom in the native substrate, is 2.9 and 2.6 Å from the switch I Asn^{229} Nδ atom and the amide nitrogen of the P-loop Gly^{108}, respectively. The elongated conformation of the switch I loop, described above, allows Asn^{229} to approach the atomic β-γ bridging substitute. In the Eg5·ADP structure, the compara-

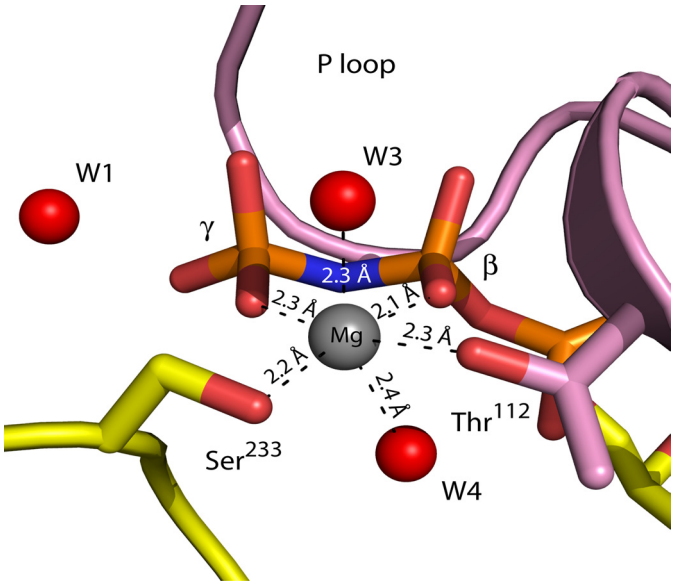

FIGURE 4. **Coordination of the Mg^{2+} ion.** The Mg^{2+} ion is tightly coordinated by oxygen atoms of the β- and γ-phosphate, Ser^{233} of switch I, Thr^{112} of the P-loop, and two water molecules. The ion location is quite similar to that seen in the Eg5·ADP structure (18), in which the Mg^{2+} ion is coordinated by Thr^{112}, a β-phosphate oxygen atom, and four water molecules.

tively shorter switch I loop alters the location of Asn^{229} and prohibits interaction with the nucleotide. Thus, in the ATP-bound motor, closure of switch I would allow for H-bonding between Asn^{229} and the β-γ bridging oxygen, which would stabilize developing negative charge on this atom during catalysis.

The three oxygen atoms of the γ-phosphate are securely coordinated in the prehydrolysis state of this kinesin; there are at least two chemical groups within interaction distance of each γ-phosphoryl oxygen. The O1 atom of the γ-phosphate is coordinated by the N_ζ atom of the P-loop Lys^{111} and the amide nitrogen of switch II Gly^{268} (Fig. 3*b*). The O2 atom of the γ-phosphate is within hydrogen-bonding distance of the hydroxyl group of the P-loop Thr^{107} and the side chain of switch I Ser^{232}. Analogous to the Kif22·AMPPNP structure (23), the presence of the γ-phosphate elicits an alternate rotamer conformation of Thr^{107} that facilitates interaction with the γ-phosphate. In this position, Thr^{107} comprises an element of the γ-phosphate sensor, which reorients following phosphate release to form an H-bond to Glu^{270} in switch II (supplemental Movie S2). In addition, the O3 atom of the γ-phosphate is within hydrogen-bonding distance of the amide nitrogen of Ser^{233} in switch I and the Mg^{2+} ion.

The Mg^{2+} ion, required for charge stabilization in ATP hydrolysis (33), coordinates six ligands in an octahedral geometry (Fig. 4) in the Eg5·AMPPNP complex. These ligands are γ- and β-phosphoryl oxygens of the substrate mimic, the Oγ atom of switch II Ser^{233}, Oγ of the P-loop Thr^{112}, and water molecules (**W3** and **W4**). We propose that the Mg^{2+} ion secures the in-line nucleophilic attack configuration, stabilizes alterations in charge distribution between the β- and γ-phosphate moieties of the substrate, and potentially facilitates protonation of the ADP leaving group oxyanion. The latter point is supported by examination of the open nucleotide-binding site in the Eg5·ADP complex (18); Mg^{2+} becomes coordinated with two additional water molecules that displace bonds to Ser^{233} and to the γ-phosphate in the AMPPNP state.

Notably, the atomic interactions described above lead to the conclusion that the conventional function attributed to switch regions in NTPases in general is not a complete description. Switches I and II are traditionally portrayed as γ-phosphate sensors (16). Our data show that these conserved sequence elements do interact with the substrate as anticipated but are equally critical for transiently organizing both water molecules in the active site. The majority of atomic interactions involving switch I and switch II residues (Fig. 5*a*) provide charge stabilization of the nucleophilic water and **W2**, the catalytic base. The P-loop residues bind the α- and β-phosphate groups of the nucleotide and the scissile phosphate moiety (Fig. 5*a*).

DISCUSSION

This structural study provides direct experimental detection of the general base that initiates catalysis in motor proteins, a first among kinesins as well as a first among any group of protein machines that use ATP hydrolysis to drive function. The major surprise of this work on kinesin proteins is the strong correspondence of the mechanistic observations in our experimentally derived structure to hypothetical and calculated models of NTP hydrolysis in other classes of proteins. Multiple waters have been postulated to be favorable in the F_1-ATPase through mutational analysis (34) and computational efforts (35) and in myosin via remarkably consistent theoretical studies (36). Multiple waters have previously been experimentally observed in $p21^{ras}$ (31), although in quite a different spatial organization from this study. Coupled with our data, this detection of waters in the G-protein active site opens the door for the argument that the chemical nature of the catalytic base is conserved in other P-loop NTPases.

Our data provide new information beyond the theoretical studies published and serve as a powerful aid in building a description of the initial reaction steps that are likely to occur within the kinesin active site. Questions we will address are (i) the general mechanism of nucleotide hydrolysis for motor proteins, (ii) the catalytic role of the waters present in the active site, and (iii) the cause-and-effect link by which active site reactions are transmitted to distal sites. ATP hydrolysis is proposed to proceed through either of two general mechanisms (37–40): dissociative or associative. A dissociative mechanism occurs when the β-γ bond of ATP is cleaved prior to binding of the nucleophilic water to the γ-phosphorus. This mechanism would involve development of a negative charge on the bridging oxygen and an HPO_3^- intermediate. In contrast, an associative mechanism features bond formation between the nucleophilic water and the γ-phosphorus, creating a pentacoordinate transition state that destabilizes the β-γ bond, leading to bond cleavage. In this case, negative charge would develop on the γ-phosphate.

These hydrolytic mechanisms can be distinguished by examining distances between the γ-phosphorus atom and the attacking and leaving group oxygens, the γ-phosphate geometry, and charge stabilization of the γ- *versus* β-phosphate. An associative mechanism requires the close approach of the attacking nucleophile (41), and distances as short as 2.7 Å between the

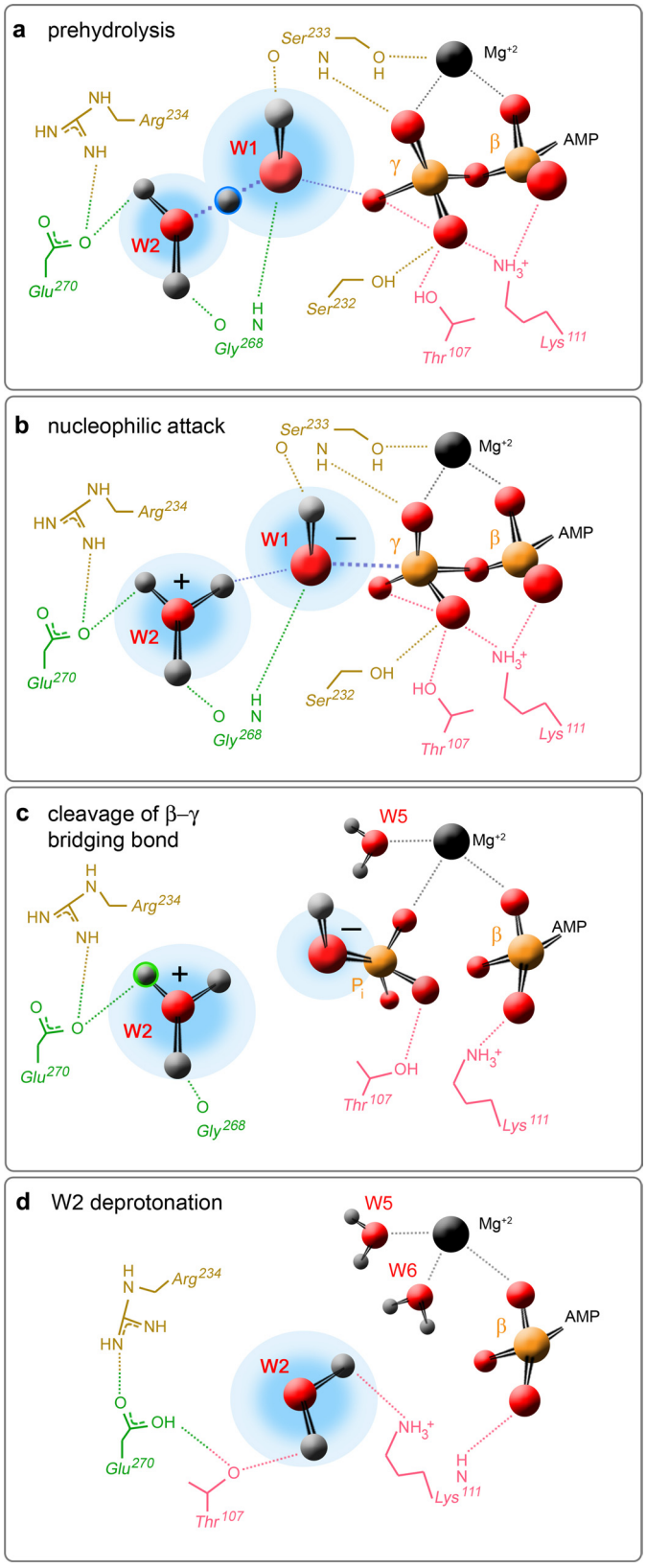

FIGURE 5. **Proposed model of ATP hydrolysis.** Four different mechanistic steps are postulated for this human kinesin-5 motor domain: *a*, the prehydrolysis state, in which there is deprotonation of the nucleophilic water by **W2**; *b*, nucleophilic attack of the scissile phosphate of ATP; *c*, cleavage of the β-γ-phosphoanhydride bond; and *d*, deprotonation of **W2** by Glu^{270}. Shown are residues from switch I (*tan*), switch II (*green*), and the P-loop (*pink*) that coordinate **W1**, **W2**, and the β- and γ-phosphates of the substrate in the prehydrolysis state. Also shown are three of the interactions for the divalent cation (*black sphere*). Atomic details in *b* and *c* are speculative and are hypothetical interactions for residues shown in *panel a*. The atomic details in *d* reflect only a subset of the interactions reported for the Eg5·ADP structure (18).

nucleophilic water and the γ-phosphorus are indicative of this reaction pathway (17). In contrast, distances as long as 5.3 Å (42) between these two atoms are reflective of a dissociative reaction. In our structure, **W1** is 3.3 Å from the γ-phosphorus atom and 2.9 Å from O2 of the γ-phosphate, distances supporting an associative mechanism (Fig. 3*a*). Additionally, **W1** is in a near equidistant position from all three γ-phosphate oxygens, a geometry favoring formation of a pentacoordinated intermediate and in-line nucleophilic attack. Finally, as discussed previously, there is extensive charge stabilization of the γ-phosphate of the AMPPNP. In contrast, contacts with the bridging oxygen, limited to Asn^{229} and the backbone carbonyl of Gly^{108}, are not likely to foster accumulation of negative charge in preparation for a dissociative mechanism. Based on these observations, our data favor the conclusion that the prehydrolysis state of Eg5 kinesin is primarily associative in character.

The second major question we address is the catalytic role of the two waters present in the active site of Eg5·AMPPNP. Foremost, these water molecules are recruited as critical chemical reagents. They are the key players in the hydrolysis reaction: the nucleophile (**W1**) that transfers its negative charge to the substrate and the catalytic base (**W2**) that accepts the proton (Fig. 5*a*). This transient water bridge can shuttle protons rapidly across the solvent H-bonds and delocalize their charge. The observed 2.4 Å distance between the oxygens of **W1** and **W2** (Fig. 3), uncommonly small for any structure despite allowance for noise in the diffraction experiment, is diagnostic for the protonation state of these solvent molecules. Although x-ray diffraction methods are not traditionally associated with observing protons, proton transfer is exquisitely dependent on structure; as the distance a proton can tunnel is less than a covalent bond length, atoms participating in the acid-base catalysis must be in quite close proximity.

In other protein structures (43), representative distances between oxygens of adjacent water molecules are significantly larger at nearly 2.8 Å, suggesting that **W1**–**W2** in the Eg5 orthosteric site are not in the ground state. Reported O–O distances that approximate our **W1**–**W2** pair are 2.55, 2.45, and 2.4 Å, measured between a water molecule and a protonated hydronium ion (44), a hydroxide ion (45), and a shared proton with a second water molecule (46), respectively. We deduce that a proton is localized and shared between the water pair in this crystal structure of the Eg5 prehydrolysis state and that proton abstraction from the nucleophile is facilitated via a Grotthuss-type mechanism (47). Real-time monitoring of Eg5 kinesin catalysis[3] corroborates that a delocalized proton within a water cluster is observed. As the abstracted proton on **W2** creates a hydronium ion (Fig. 5*b*), the switch II Glu^{270} carboxylate can provide the required charge stabilization for the pos-

[3] B. Jun and S. Kim, manuscript in preparation.

itively charged hydronium ion via complex salt-bridge formation (Fig. 5*b*).

The **W1–W2** proton relay network is the central cause-and-effect link between chemistry and conformational changes distal from the orthosteric site and critical for motor protein function. Unlike other catalytic reaction mechanisms, the second protonation event in the Eg5 active site is equally important as the first. A second proton transfer from the **W2** hydronium ion to Glu^{270} will destabilize the interswitch Glu^{270}–Arg^{234} salt bridge. Breaking the H-bond between this residue pair will result in conformational changes in the switch I and switch II regions that lead to opening of the active site (Fig. 5*d*). Thus, the scission of the interswitch Arg^{234}–Glu^{270} salt bridge is the basis for local chemical modifications amplifying into structural rearrangements. Subsequently, the open nucleotide-binding cavity may allow P_i release and permit reorientation of the Thr^{107} side chain to move within 2.4 Å of Glu^{270} (Fig. 5*d*), re-establishing an interaction seen in the Eg5·ADP structure (18). Environmentally sensitive salt-bridge structures are known to play an important role in biological systems and act as controllable switches participating in various gating mechanisms. The hydrogen-bonded ion pair is required for efficient and synchronized motor function (15), and this simple salt bridge can stabilize the closed conformation in Eg5 kinesin (18). Our data provide a mechanistic rationale for kinesins and perhaps ATPases in general.

Usage of protonated water clusters in protein machines capable of NTP hydrolysis is equivalent in importance to the role of transition state stabilization through electrostatics or H-bonding. Biochemically, this **W1–W2** cluster forms an H-bonding network that lifts the constraint of an acid-base pair being in close proximity; a shuttled proton along the water cluster can communicate chemical modification of the scissile phosphate to regions of the protein distant from the substrate. Functionally, an H-bonded water network permits communication with a larger number of switch regions in the protein and can trigger a greater range of conformational changes distant from the active site and required for force production and movement. These mechanistic outcomes would be unachievable with a single proton transfer event or one active site water.

Important for its cellular role, control of the direction and reversibility of proton transfer can be realized with this orthosteric water cluster in tandem with a terminal salt bridge at the edge of the motor domain active site. Metamorphosis from a simple to a **W2**-complexed salt bridge results in minor, stepwise changes in geometry as the Arg^{234}–Glu^{270} interaction in kinesin is already constrained. Moreover, the organization and chemistry of the active site players permit reversibility in kinesin catalysis. The **W1** and **W2** are equivalently amphiprotic, can both accept and donate protons, and can allow the same Grotthuss-type mechanism (47) to proceed in either direction. Similar bidirectionality of transfer can be constructed with other, adjacent amphiprotic species, such as the neighboring Ser^{232} and Ser^{233} residues in switch I. We speculate that motor proteins may have repeated the use of this theme in their catalytic sites at the level of both protein and solvent to ensure control of catalytic commitment and coordination with events at the cytoskeletal-binding site.

Acknowledgments—We are grateful to Richard Walker, Arthur Haas, Charles F. Yocum, Eran Pichersky, and Rebecca Ward for providing comments on this manuscript. Elizabeth D. Kim and Catherine D. Kim assisted in generating Fig. 5.

REFERENCES

1. Endow, S. A. (1999) *Eur. J. Biochem.* **262,** 12–18
2. Hirokawa, N. (1998) *Science* **279,** 519–526
3. Fisher, A. J., Smith, C. A., Thoden, J. B., Smith, R., Sutoh, K., Holden, H. M., and Rayment, I. (1995) *Biochemistry* **34,** 8960–8972
4. Gulick, A. M., Bauer, C. B., Thoden, J. B., and Rayment, I. (1997) *Biochemistry* **36,** 11619–11628
5. Onishi, H., Mochizuki, N., and Morales, M. F. (2004) *Biochemistry* **43,** 3757–3763
6. Wojcik, E. J., Dalrymple, N. A., Alford, S. R., Walker, R. A., and Kim, S. (2004) *Biochemistry* **43,** 9939–9949
7. Navaza, J. (1994) *Acta Crystallogr. Sect. A* **50,** 157–163
8. Brünger, A. T., Adams, P. D., Clore, G. M., DeLano, W. L., Gros, P., Grosse-Kunstleve, R. W., Jiang, J. S., Kuszewski, J., Nilges, M., Pannu, N. S., Read, R. J., Rice, L. M., Simonson, T., and Warren, G. L. (1998) *Acta Crystallogr D Biol Crystallogr.* **54,** 905–921
9. Jones, T. A., Zou, J. Y., Cowan, S. W., and Kjeldgaard, M. (1991) *Acta Crystallogr. Sect. A* **47,** 110–119
10. Collaborative Computational Project, Number 4 (1994) *Acta Crystallogr D Biol Crystallogr.* **50,** 760–763
11. Kleywegt, G. J., and Jones, T. A. (1998) *Acta Crystallogr. D Biol. Crystallogr.* **54,** 1119–1131
12. DeLano, W. L. (2008) *The PyMOL Molecular Graphics System*, DeLano Scientific LLC, Palo Alto, CA
13. Hodis, E., Schreiber, G., Rother, K., and Sussman, J. L. (2007) *Trends Biochem. Sci* **32,** 199–204
14. Kikkawa, M., and Hirokawa, N. (2006) *EMBO J.* **25,** 4187–4194
15. Kull, F. J., and Endow, S. A. (2002) *J. Cell Sci.* **115,** 15–23
16. Vale, R. D. (1996) *J. Cell Biol.* **135,** 291–302
17. Smith, C. A., and Rayment, I. (1996) *Biochemistry* **35,** 5404–5417
18. Turner, J., Anderson, R., Guo, J., Beraud, C., Fletterick, R., and Sakowicz, R. (2001) *J. Biol. Chem.* **276,** 25496–25502
19. Kikkawa, M. (2008) *Trends Cell Biol.* **18,** 128–135
20. Woehlke, G., Ruby, A. K., Hart, C. L., Ly, B., Hom-Booher, N., and Vale, R. D. (1997) *Cell* **90,** 207–216
21. Bodey, A. J., Kikkawa, M., and Moores, C. A. (2009) *J. Mol. Biol.* **388,** 218–224
22. Sindelar, C. V., and Downing, K. H. (2007) *J. Cell Biol.* **177,** 377–385
23. Cochran, J. C., Sindelar, C. V., Mulko, N. K., Collins, K. A., Kong, S. E., Hawley, R. S., and Kull, F. J. (2009) *Cell* **136,** 110–122
24. Furch, M., Fujita-Becker, S., Geeves, M. A., Holmes, K. C., and Manstein, D. J. (1999) *J. Mol. Biol.* **290,** 797–809
25. Onishi, H., Kojima, S., Katoh, K., Fujiwara, K., Martinez, H. M., and Morales, M. F. (1998) *Proc. Natl. Acad. Sci. U.S.A.* **95,** 6653–6658
26. Onishi, H., Ohki, T., Mochizuki, N., and Morales, M. F. (2002) *Proc. Natl. Acad. Sci. U.S.A.* **99,** 15339–15344
27. Nitta, R., Kikkawa, M., Okada, Y., and Hirokawa, N. (2004) *Science* **305,** 678–683
28. Ogawa, T., Nitta, R., Okada, Y., and Hirokawa, N. (2004) *Cell* **116,** 591–602
29. Dittrich, M., and Schulten, K. (2005) *J. Bioenerg. Biomembr.* **37,** 441–444
30. Grigorenko, B. L., Rogov, A. V., Topol, I. A., Burt, S. K., Martinez, H. M., and Nemukhin, A. V. (2007) *Proc. Natl. Acad. Sci. U.S.A.* **104,** 7057–7061
31. Scheidig, A. J., Burmester, C., and Goody, R. S. (1999) *Structure* **7,** 1311–1324
32. Yang, Y., and Cui, Q. (2009) *J. Phys. Chem. A* **113,** 12439–12446
33. Kuznetsov, S. A., and Gelfand, V. I. (1986) *Proc. Natl. Acad. Sci. U.S.A.* **83,** 8530–8534
34. Ahmad, Z., and Senior, A. E. (2004) *J. Biol. Chem.* **279,** 46057–46064
35. Dittrich, M., Hayashi, S., and Schulten, K. (2004) *Biophys. J.* **87,**

2954–2967
36. Li, G., and Cui, Q. (2004) *J. Phys. Chem. B* **108,** 3342–3357
37. Maegley, K. A., Admiraal, S. J., and Herschlag, D. (1996) *Proc. Natl. Acad. Sci. U.S.A.* **93,** 8160–8166
38. Schweins, T., and Warshel, A. (1996) *Biochemistry* **35,** 14232–14243
39. Aqvist, J., Kolmodin, K., Florian, J., and Warshel, A. (1999) *Chem. Biol.* **6,** R71–80
40. Kamerlin, S. C., Florián, J., and Warshel, A. (2008) *Chem. Phys. Chem.* **9,** 1767–1773
41. Wittinghofer, A. (2006) *Trends Biochem. Sci.* **31,** 20–23
42. Granot, J., Mildvan, A. S., Bramson, H. N., and Kaiser, E. T. (1980) *Biochemistry* **19,** 3537–3543
43. Bergmann, E. M., Mosimann, S. C., Chernaia, M. M., Malcolm, B. A., and James, M. N. (1997) *J. Virol.* **71,** 2436–2448
44. Sagnella, D. E., and Voth, G. A. (1996) *Biophys. J.* **70,** 2043–2051
45. Asthagiri, D., Pratt, L. R., Kress, J. D., and Gomez, M. A. (2004) *Proc. Natl. Acad. Sci. U.S.A.* **101,** 7229–7233
46. Asthagiri, D., Pratt, L. R., and Kress, J. D. (2005) *Proc. Natl. Acad. Sci. U.S.A.* **102,** 6704–6708
47. Cukierman, S. (2006) *Biochim. Biophys. Acta* **1757,** 876–885